



**HAL**  
open science

## Ultrafast ultrasound coupled with cervical magnetic stimulation for non-invasive and non-volitional assessment of diaphragm contractility

Thomas Poulard, Martin Dres, Marie-Cécile Nierat, Isabelle Rivals, Jean-Yves Hogrel, Thomas Similowski, Jean-Luc Gennisson, Damien Bachasson

### ► To cite this version:

Thomas Poulard, Martin Dres, Marie-Cécile Nierat, Isabelle Rivals, Jean-Yves Hogrel, et al.. Ultrafast ultrasound coupled with cervical magnetic stimulation for non-invasive and non-volitional assessment of diaphragm contractility. *The Journal of Physiology*, 2020, 598 (24), pp.5627-5638. 10.1113/JP280457 . hal-03266752

**HAL Id: hal-03266752**

**<https://hal.sorbonne-universite.fr/hal-03266752>**

Submitted on 22 Jun 2021

**HAL** is a multi-disciplinary open access archive for the deposit and dissemination of scientific research documents, whether they are published or not. The documents may come from teaching and research institutions in France or abroad, or from public or private research centers.

L'archive ouverte pluridisciplinaire **HAL**, est destinée au dépôt et à la diffusion de documents scientifiques de niveau recherche, publiés ou non, émanant des établissements d'enseignement et de recherche français ou étrangers, des laboratoires publics ou privés.

The Journal of Physiology

<https://jp.msubmit.net>

**JP-TFP-2020-280457R2**

**Title:** Ultrafast ultrasound coupled with cervical magnetic stimulation for non-invasive and non-volitional assessment of diaphragm contractility

**Authors:** Thomas Poulard  
Martin Dres  
Marie-Cécile Nierat  
Isabelle Rivals  
Jean-Yves Hogrel  
Thomas Similowski  
Jean-Luc Gennisson  
Damien Bachasson

**Author Conflict:** Martin Dres: MD received personal fees from Lungpacer. Jean-Luc Gennisson: JLG is a scientific consultant for Supersonic Imagine, Aix-en-Provence, France.

**Author Contribution:** Thomas Poulard: Conception or design of the work; Acquisition or analysis or interpretation of data for the work; Drafting the work or revising it critically for important intellectual content; Final approval of the version to be published; Agreement to be accountable for all aspects of the work Martin Dres: Conception or design of the work; Drafting the work or revising it critically for important intellectual content; Final approval of the version to be published; Agreement to be accountable for all aspects of the work Marie-Cécile Nierat: Conception or design of the work; Drafting the work or revising it critically for important intellectual content; Final approval of the version to be published; Agreement to be accountable for all aspects of the work

**Disclaimer:** This is a confidential document.

Isabelle Rivals: Acquisition or analysis or interpretation of data for the work; Drafting the work or revising it critically for important intellectual content; Final approval of the version to be published; Agreement to be accountable for all aspects of the work  
Jean-Yves Hogrel: Conception or design of the work; Drafting the work or revising it critically for important intellectual content; Final approval of the version to be published; Agreement to be accountable for all aspects of the work  
Thomas Similowski: Conception or design of the work; Drafting the work or revising it critically for important intellectual content; Final approval of the version to be published; Agreement to be accountable for all aspects of the work  
Jean-Luc Gennisson: Conception or design of the work; Acquisition or analysis or interpretation of data for the work; Drafting the work or revising it critically for important intellectual content; Final approval of the version to be published; Agreement to be accountable for all aspects of the work  
Damien Bachasson: Conception or design of the work; Acquisition or analysis or interpretation of data for the work; Drafting the work or revising it critically for important intellectual content; Final approval of the version to be published; Agreement to be accountable for all aspects of the work

**Running Title:** Ultrafast ultrasound imaging of the diaphragm

**Dual Publication:** No

**Funding:** Fondation EDF: Thomas Poulard, Jean-Yves Hogrel, Damien Bachasson, N/A; Association Francaise contre les Myopathies (Association Française contre les Myopathies): Thomas Poulard, Jean-Yves Hogrel, Damien Bachasson, N/A The PhD fellowship of TP is funded by the Fondation EDF that is supporting the RespiMyo project, which includes the current study. This study was also supported by the Association Française Contre Les Myopathies (AFM).

1 **Ultrafast ultrasound coupled with cervical magnetic**  
2 **stimulation for non-invasive and non-volitional**  
3 **assessment of diaphragm contractility**

4 Thomas Poulard<sup>1,2</sup>, Martin Dres<sup>3,4</sup>, Marie-Cécile Niérat<sup>3</sup>, Isabelle Rivals<sup>5</sup>, Jean-Yves  
5 Hogrel<sup>2</sup>, Thomas Similowski<sup>3,4</sup>, Jean-Luc Gennisson<sup>1#</sup>, Damien Bachasson<sup>2#\*</sup>

6 *# equally contributing authors*

7

8

9 <sup>1</sup> Laboratoire d'Imagerie Biomédicale Multimodale, BioMaps, Université Paris-Saclay,  
10 CEA, CNRS UMR 9011, Inserm UMR1281, SHFJ, 4 place du général Leclerc, 91401, Orsay,  
11 France

12 <sup>2</sup> Institute of Myology, Neuromuscular Investigation Center, Neuromuscular Physiology  
13 Laboratory, Paris, France

14 <sup>3</sup> Sorbonne Université, INSERM, UMRS1158 Neurophysiologie respiratoire expérimentale  
15 et clinique, Paris, France

16 <sup>4</sup> AP-HP. Sorbonne Université, Hôpital Pitié-Salpêtrière, Service de Pneumologie, Médecine  
17 intensive – Réanimation (Département "R3S"), F-75013, Paris, France

18 <sup>5</sup> Equipe de Statistique Appliquée, ESPCI Paris, PSL Research University, UMRS 1158, 10  
19 rue Vauquelin, 75005, Paris, France

20

21 \*Corresponding author: Damien Bachasson, PhD. Institut de Myologie, Laboratoire de  
22 Physiologie et d'Evaluation Neuromusculaire, Hôpital Universitaire Pitié Salpêtrière, Paris  
23 75651 Cedex 13, France. Tel: +33 1 42 16 66 41; fax: +33 1 42 16 58 81. E-mail:  
24 [d.bachasson@institut-myologie.org](mailto:d.bachasson@institut-myologie.org)

25 **Table of contents categories**

26 Respiratory

27

28 **Key points summary**

29 • Twitch transdiaphragmatic pressure elicited by cervical magnetic stimulation of the  
30 phrenic nerves is a fully non-volitional method for assessing diaphragm contractility  
31 in humans, yet it requires invasive procedures such as esophageal and gastric catheter-  
32 balloons.

33 • Ultrafast ultrasound enables a very high frame rate allowing the capture of transient  
34 events, such as muscle contraction elicited by nerve stimulation (twitch). Whether  
35 indices derived from ultrafast ultrasound can be used as an alternative to the invasive  
36 measurement of twitch transdiaphragmatic pressure is unknown.

37 • Our findings demonstrate that maximal diaphragm tissue velocity assessed using  
38 ultrafast ultrasound following cervical magnetic stimulation is reliable, sensitive to  
39 change in cervical magnetic stimulation intensity, and correlates to twitch  
40 transdiaphragmatic pressure.

41 • This approach provides a novel fully non-invasive and non-volitional tool for the  
42 assessment of diaphragm contractility in humans.

43 **Abstract**

44 Measuring twitch transdiaphragmatic pressure ( $P_{di_{tw}}$ ) elicited by cervical magnetic  
45 stimulation (CMS) is considered as a reference method for the standardized evaluation of  
46 diaphragm function. Yet, the measurement of  $P_{di}$  requires invasive esophageal and gastric  
47 catheter-balloons. Ultrafast ultrasound is a non-invasive imaging technique enabling frame  
48 rates high enough to capture transient events such as evoked muscle contractions. This study  
49 investigated relationships between indices derived from ultrafast ultrasounds and  $P_{di_{tw}}$ , and  
50 how these indices may be used to estimate  $P_{di_{tw}}$ . CMS was performed in 13 healthy  
51 volunteers from 30 to 100 % of stimulator intensity in units of 10 % in a randomized order.  
52  $P_{di_{tw}}$  was measured and the right hemidiaphragm was imaged using a custom ultrafast  
53 ultrasound sequence with 1 kHz framerate. Maximal diaphragm axial velocity ( $V_{di_{max}}$ ) and  
54 diaphragm thickening fraction ( $TF_{di_{tw}}$ ) were computed. Intra-session reliability was  
55 assessed. Repeated-measures correlation ( $R$ ) and Spearman correlation coefficients ( $\rho$ ) were  
56 used to assess relationships between variables. Intra-session reliability was strong for  $P_{di_{tw}}$   
57 and  $V_{di_{max}}$  and moderate for  $TF_{di_{tw}}$ .  $V_{di_{max}}$  correlated with  $P_{di_{tw}}$  in all subjects ( $0.64 < \rho <$   
58  $1.00$ ,  $R = 0.75$ ; all  $p < 0.05$ ).  $TF_{di_{tw}}$  correlated with  $P_{di_{tw}}$  in 8 subjects only ( $0.85 < \rho < 0.93$ ,  
59  $R = 0.69$ ; all  $p < 0.05$ ). Coupling ultrafast ultrasound and CMS show promise for the non-  
60 invasive and fully non-volitional assessment of diaphragm contractility. This approach opens  
61 up prospects for both diagnosis and follow-up of diaphragm contractility in clinical  
62 populations.

63

64 **Key Words:** Diaphragm, ultrafast ultrasound imaging, cervical magnetic stimulation,  
65 skeletal muscle, contractility, phrenic nerves

## 66 Introduction

67 Sixty years ago, [Agostoni & Rahn, \(1960\)](#) introduced a novel method to measure the  
68 specific contribution of the diaphragm to the intrathoracic pressure generated during  
69 inspiratory efforts, namely, transdiaphragmatic pressure (Pdi). Pdi is defined as the difference  
70 between gastric (Pga) and esophageal (Pes) pressures measured using gastric and esophageal  
71 probes. Twitch Pdi ( $P_{di_{tw}}$ ) elicited by cervical magnetic stimulation (CMS) was introduced  
72 30 years ago and is considered as a reference method for the non-volitional assessment of  
73 diaphragm contractility ([Similowski et al., 1989](#)). Yet, measuring  $P_{di_{tw}}$  is considered invasive  
74 and requires a high level of expertise ([Laveneziana et al., 2019](#)). Twitch mouth pressure  
75 ( $P_{mo_{tw}}$ ) or nasal mask twitch pressure have been developed as an alternative to  $P_{di_{tw}}$  ([Yan et](#)  
76 [al., 1992](#); [Teixeira et al., 2007](#)). However, this approach requires some degree of cooperation  
77 from the subjects because small inspiratory/expiratory efforts ([Similowski et al., 1993](#);  
78 [Hamnegaard et al., 1995](#); [Windisch et al., 2005](#); [Kabitz et al., 2007](#)) are required prior the  
79 stimulation to prevent upper airway collapse and/or glottis closure and ensure adequate  
80 transmission. Moreover, these procedures required proper mouth occlusion, which cannot be  
81 performed in many patients such as patients with neuromuscular disorders.

82 Ultrasound (US) imaging has emerged as a tool for assessing the diaphragm ([Ueki et](#)  
83 [al., 1995](#)) and is increasingly used in clinical settings such as the intensive care unit ([Dres &](#)  
84 [Demoule, 2020](#)). Imaging of the zone of apposition of the right-hemidiaphragm is classically  
85 performed to investigate diaphragm behavior. Various indices can be derived from  
86 diaphragm US such as diaphragm excursion or thickening fraction ([Goligher et al., 2015](#);  
87 [Tuinman et al., 2020](#)), diaphragm strain ([Oppersma et al., 2017](#)), or more recently changes  
88 in diaphragm stiffness assessed with US shear wave elastography ([Bachasson et al., 2019](#)).  
89 However, these methods offer limited frame rate (i.e. a few tens of frames per second for  
90 standard US and a few frames per second for US shear wave elastography). Therefore, these  
91 methods cannot be used for capturing fast transient phenomena, such as diaphragm response  
92 elicited by CMS (~300 ms).

93 Ultrafast US is a fairly recent imaging technique enabling very high frame rates (up  
94 to 20 kHz, ([Sandrin et al., 1999](#)). This technique has previously been used in the biceps

95 brachii to visualize muscle behavior during short-lasting contractions ([Deffieux et al., 2008](#);  
96 [Gronlund et al., 2013](#)). By performing a radio frequency-based speckle tracking, ultrafast US  
97 allows the quantification of transient velocities of mechanical waves induced by  
98 transcutaneous electrical stimulation ([Deffieux et al., 2008](#)). Maximal tissue velocity has  
99 been reported to increase linearly with stimulation intensity. However, the relationship  
100 between tissue velocity and the force generated by the muscle during stimulation is unknown.  
101 In a recent pilot work, we reported that diaphragm response elicited by CMS can be imaged  
102 using ultrafast US and that responses elicited at high and low stimulation intensity can be  
103 discriminated ([Bachasson et al., 2018](#)). However, the relationship between diaphragm  
104 pressure generation and indices derived from ultrafast US during CMS remains to be  
105 thoroughly investigated.

106 Therefore, this study aimed at imaging the diaphragm during CMS at different  
107 intensity levels using ultrafast US. By investigating the relationships between  $P_{di_{tw}}$  and  
108 indices derived from ultrafast US imaging (i.e. thickening fraction, maximal tissue velocity),  
109 we hypothesized that diaphragm thickening fraction and diaphragm tissue velocity following  
110 CMS were correlated to  $P_{di_{tw}}$ , and that these indices may be used as a surrogate to  $P_{di_{tw}}$ .

## 111 **Methods**

### 112 **Ethical approval**

113 This study conformed to the Declaration of Helsinki. It was approved by the local  
114 ethics committee (Comité de Protection des Personnes Île-de-France VI, France, February  
115 22<sup>nd</sup> 2016, ID-RCB 2015-A00949-40) and was publicly registered before the first inclusion  
116 (ClinicalTrials.gov, NCT03313141). All participants gave written informed consent. Some  
117 of the data from this study have already been published elsewhere, regarding the use of  
118 diaphragm shear wave elastography in healthy subjects during ventilation ([Bachasson et al.,  
119 2019](#)).

### 120 **Participants**



## Ultrafast ultrasound imaging of the diaphragm

121 Thirteen healthy participants (5 males and 8 females, median (Q1-Q3) – age = 24 (22-  
122 27) years, height = 171 (167-183) cm, BMI = 20.6 (19.7-22.6) kg.m<sup>-2</sup>) were studied.  
123 Participants had to be 18 and over with no history of respiratory or neuromuscular disorders,  
124 and no contraindication to CMS ([Rossi et al., 2011](#)).

### 125 **Pressure measurements**

126 Participants were studied in a semirecumbent position (~45 degrees) with uncast  
127 abdomen. Pes and Pga were measured using 8 cm balloon catheters (Marquat Genie  
128 Biomedical, Boissy-Saint-Léger Cedex, France). Balloons were introduced through the  
129 participant's nostril and both placed in the stomach so that a positive pressure deflection was  
130 monitored when gently pressing the participant's stomach. Subsequently, one balloon was  
131 slowly withdrawn toward the esophagus until the pressure deflection was no more monitored  
132 when pressing the participant's stomach, and was then withdrawn an additional 10 cm.  
133 Esophageal balloon position was adjusted using the Baydur maneuver ([Baydur et al., 1982](#)).  
134 Balloons were then connected to differential pressure transducers (MLT0380/D,  
135 ADInstruments, Bella Vista, Australia) and filled with 4 and 5.5 ml of air in the esophageal  
136 and gastric balloons, respectively ([Mojoli et al., 2015](#)). All signals were digitized at a 4 kHz  
137 frequency using a PowerLab system (16/35, ADInstruments, Bella Vista, Australia) and  
138 recorded on the LabChart software. Pdi was computed as the difference between Pga and  
139 Pes.

### 140 **Cervical Magnetic Stimulation**

141 CMS was performed using a Magstim 200 stimulator (Magstim, Whitland, Dyfed,  
142 UK) driving a 90-mm circular coil (1 Tesla maximum output) as previously described  
143 ([Similowski et al., 1989](#)). Briefly, participants were asked to bend their neck forward and the  
144 central hole of the coil was positioned on the spinous process of the seventh cervical vertebra.  
145 Optimal coil position was determined by performing a series of stimulation at 100 % of  
146 stimulator intensity. The spot where Pdi<sub>tw</sub> was the highest was skin-marked and kept constant  
147 during the whole experiment.

### 148 **Ultrafast ultrasound imaging**

149           The zone of apposition of the right hemidiaphragm was imaged using a 6 MHz central  
150 frequency linear transducer (SL 10-2) driven by an ultrafast ultrasound device (Aixplorer  
151 V12, Supersonic Imagine, Aix-en-Provence, France). The probe was placed on the mid-  
152 axillary line, vertical to the chest wall, at the 8th-10th intercostal space. The site of the probe  
153 placement was skin-marked to ensure that the same region of interest was imaged during the  
154 whole protocol. The diaphragm was identified as a three-layers structure superficial to the  
155 liver, with two hyperechoic layers (*i.e.* the *pleura* and *peritoneum*) surrounding a hypoechoic  
156 muscular layer (Figure 1). As the duration of  $P_{di_{tw}}$  is  $\sim 300$  ms, a custom ultrafast US  
157 sequence was designed to track diaphragm movements during this time window. The  
158 sequence was composed of 9 plane-wave US with different angles ( $-7^\circ$  to  $7^\circ$  with a  $2^\circ$   
159 incremental steps) at 9 kHz frame rate, yielding a compounded frame rate of 1 kHz and a 500  
160 ms ([Montaldo et al., 2009](#)). This sequence followed the Food and Drugs Administration  
161 guidelines for acoustics norms (Mechanical index = 0.5, Thermal index = 0.2). Because  
162 diaphragm depth rarely exceed 4 cm ([Shahgholi et al., 2014](#)), the US sequence was developed  
163 in order to maintain the same spatial and temporal resolution of to this depth of 4 cm. Such  
164 sequence allows the imaging of the diaphragm in overweight patients. Signals were  
165 synchronized using an output trigger sent from the ultrafast US device to the Powerlab  
166 system. A fixed delay of 100 ms was set between the onset of US recordings and CMS, after  
167 which the stimulator was triggered by the Powerlab for delivering the stimulation. Recording  
168 of pressure signals was started 1 s before the US trigger. The experimental setup and  
169 procedure for recording pressure and US frames is displayed in Figure 2. Of note, we  
170 investigated whether diaphragm excursion elicited by CMS may be imaged during subcostal  
171 scanning during pilot works. We measured very small excursion values that were highly  
172 variable between trials. This finding was expected as diaphragm response elicited by CMS  
173 is not associated with substantial change in pulmonary volume. This may be mainly  
174 explained by glottis closure. Consequently, the measurement of diaphragm excursion during  
175 CMS was not further explored.

### 176 **Experimental protocol**

177 *Cervical magnetic stimulations.* Participants were stimulated on the predefined optimal  
178 stimulation spot from 30 to 100 % of stimulator intensity in units of 10 %, in a randomized  
179 order. All stimulations were delivered at functional residual capacity (FRC). Lung volume  
180 prior stimulation, estimated through Pes, was checked to be consistent across all stimulations.  
181 A minimum of three stimulations, separated by at least one minute, were performed at each  
182 stimulation intensity. Two to three validated trials (i.e. as indicated by appropriate Pes before  
183 CMS) per intensity were considered for further analysis.

184 *Maximal voluntary maneuvers.* Participants were asked to perform maximal inspiratory  
185 effort at residual volume. Maximal Pdi ( $P_{di_{max}}$ ) was measured using a unidirectional valve  
186 allowing expiration only. Participants were asked to empty their lungs before being strongly  
187 encouraged to generate maximal inspiratory effort. Visual feedback of Pdi was provided  
188 during the maneuver. Three to five trials were performed and maximal pressure measured  
189 over a 1 s period was recorded as  $P_{di_{max}}$ . Sniff nasal inspiratory pressure (SNIP) was  
190 determined as follows. Participants were asked to make a short and maximal sniff at FRC.  
191 As recommended ([American Thoracic Society/European Respiratory, 2002](#)), participants  
192 performed 8-10 attempts with a ~30-s rest in-between sniffs until a plateau of peak pressure  
193 values was reached.

#### 194 **Data analysis**

195 All data were analyzed offline using standardized Matlab scripts (Mathworks, Natick,  
196 MA, USA). Pes, Pga, and Pdi signals were low-pass filtered (30 Hz) using a second-order  
197 Butterworth filter. Esophageal twitch pressure ( $P_{es_{tw}}$ ), gastric twitch pressure ( $P_{ga_{tw}}$ ), and  
198  $P_{di_{tw}}$  following stimulation were calculated as the difference between maximal (for Pdi and  
199 Pga) or minimal (for Pes) pressure and pressure at the onset of CMS.

200 Vertical speckle tracking was performed by computing the axial (i.e. perpendicular  
201 to the ultrasound probe) relative displacements within the diaphragm. This technique consists  
202 in comparing consecutive images using one-dimensional cross-correlations to measure the  
203 relative displacement of a pixel between two consecutive frames ([Loupas et al., 1995](#)).  
204 Diaphragm tissue velocity profile is then computed by dividing the measured displacement  
205 by the time difference between two frames (i.e. 1 ms). As an example, Figure 3 shows how

206 the velocity within the diaphragm evolves over time. Diaphragm velocity was computed over  
 207 each column of pixels within the diaphragm. The central third of each image was then  
 208 averaged to obtain a single value of diaphragm velocity over time. This value was assumed  
 209 to be representative of the whole diaphragm. Maximal diaphragm velocity ( $V_{di_{max}}$ ) was then  
 210 determined as the maximal (i.e. positive) velocity within this signal.

211 For each trial, a time-motion image was generated using the central pixel line of each  
 212 ultrasound image, referred to as M-Mode in the following. The position of the *pleura* and  
 213 *peritoneum* layers was then drawn manually over the full length of the M-Mode image. By  
 214 doing so, diaphragm thickness (i.e. the difference between the *peritoneum* and *pleura*  
 215 positions) was computed at each time of the US acquisition. Maximal diaphragm thickening  
 216 fraction ( $TF_{di_{tw}}$ ) was computed using resting diaphragm thickness prior stimulation ( $T_{di_{rest}}$ )  
 217 and maximal diaphragm thickness following stimulation ( $T_{di_{max}}$ ) as follows:

$$218 \quad TF_{di_{tw}} (\%) = \frac{T_{di_{max}} - T_{di_{rest}}}{T_{di_{rest}}} \times 100 \quad [1]$$

219 All  $TF_{di_{tw}}$  measurements were performed by a single trained operator (TP), blinded to the  
 220 stimulation intensity. A movie clip showing pressure signals, M-mode images, and indices  
 221 derived from ultrafast US is available in supplementary materials S1.

## 222 **Statistics**

223 Results are presented as median (Q1-Q3) unless otherwise stated. Normality was assessed by  
 224 visual inspection (*QQ plots* and density distributions) and by significance tests (*Shapiro-Wilk*  
 225 *test*). Because all variables failed the normality test, Friedman repeated measures ANOVAs  
 226 were used. ANOVAs were conducted to compare  $P_{di}$  prior to each stimulation at all  
 227 stimulation intensities. Within-day reliability of  $P_{di_{tw}}$ ,  $V_{di_{max}}$ , and  $TF_{di_{tw}}$  was investigated.  
 228 Standard errors of measurement (SEM) and intraclass correlation coefficients (ICC) were  
 229 used to study absolute and relative reliability, respectively ([Hopkins, 2002](#)). The overall  
 230 relationship between variables (R) was determined using repeated measure correlation  
 231 ([Bakdash & Marusich, 2017](#)). This technique considers the independence of repeated  
 232 measures between individuals, so that potential confounding factors, such as between-  
 233 participant variability, do not interfere. Data are presented as R [95 % CI]. Spearman

234 correlation coefficients ( $\rho$ ) were calculated to investigate within-individual relationships  
 235 between variables. ANOVAs were used to assess the effect of stimulation intensity on Pdi<sub>tw</sub>,  
 236 Vdi<sub>max</sub>, and TFdi<sub>tw</sub>. Tukey's *post-hoc* tests were conducted if a significant main effect of  
 237 intensity was found. Within individuals, Pdi<sub>tw</sub>, Vdi<sub>max</sub>, and TFdi<sub>tw</sub> were considered  
 238 supramaximal if the average Pdi<sub>tw</sub>, Vdi<sub>max</sub> or TFdi<sub>tw</sub> at submaximal and maximal stimulation  
 239 intensities was inferior or equal to the coefficient of variation of the variable at each  
 240 stimulation intensities ([Welch et al., 2018](#); [Geary et al., 2019](#)). Supramaximality was reached  
 241 if greater stimulation intensity did not result in further increase in Pdi<sub>tw</sub>, Vdi<sub>max</sub> or TFdi<sub>tw</sub>.  
 242 Analyses were performed in the computing environment R ([R Core Team, 2020](#)).  
 243 Significance was set at  $p < 0.05$  for all tests.

## 244 **Results**

245 All participants completed the protocol. Pdi<sub>max</sub> was 113 (71-115) cmH<sub>2</sub>O 90 (56-117)  
 246 cmH<sub>2</sub>O in men and women, respectively. Overall, Pdi<sub>max</sub> was 108 (71-117) cmH<sub>2</sub>O. SNIP  
 247 was 116 (109-130) cmH<sub>2</sub>O in men and 103 (90-118) cmH<sub>2</sub>O in women. Overall, SNIP was  
 248 109 (96-123) cmH<sub>2</sub>O. The one-way repeated measures ANOVA showed that Pes at the onset  
 249 of CMS was similar across all stimulations at all intensities ( $p = 0.2430$ ). Within-day SEM  
 250 and ICC of Pdi<sub>tw</sub>, Vdi<sub>max</sub>, and TFdi<sub>tw</sub> are presented in Table 1. Typical B-Mode images over  
 251 the course of the 500 ms US acquisition are presented in supplementary materials S2.

### 252 **Effect of stimulation intensity on indices derived from ultrafast ultrasound**

253 M-Mode images and temporal evolution of the displacements of the *pleura* and  
 254 *peritoneum*, Vdi<sub>max</sub>, and recorded pressures in one individual are displayed in Figure 4 (also  
 255 see movie clip in Supporting Information S1). Pes<sub>tw</sub>, Pga<sub>tw</sub>, and Pdi<sub>tw</sub> at all tested stimulation  
 256 intensities are shown in Figure 5 and Figure 6A. Vdi<sub>max</sub> and TFdi<sub>tw</sub> at all tested stimulation  
 257 intensities are displayed in Figure 6B-C. Within individual relationships between stimulation  
 258 intensity and Pdi<sub>tw</sub>, Vdi<sub>max</sub>, and TFdi<sub>tw</sub> are shown in Figure 6D-F.

259 Pdi<sub>tw</sub> was significantly related to stimulation intensity in all subjects ( $\rho$  ranged from  
 260 0.83 to 1.00, all  $p < 0.0100$ ;  $R = 0.91$ , 95 % CIs [0.86 0.94],  $p < 0.0001$ ). At the group level,  
 261 there was a significant main effect of stimulation intensity on Pdi<sub>tw</sub>. *Post-hoc* tests indicated

262 that  $Pdi_{tw}$  significantly increased up to 100 % of stimulation intensity (all  $p < 0.05$ ). Within  
 263 individuals,  $Pdi_{tw}$  plateaued at 90 % of stimulation intensity in two participants. In other  
 264 participants,  $Pdi_{tw}$  increased until 100 % of stimulation intensity.

265  $Vdi_{max}$  correlated to stimulation intensity in all participants ( $\rho$  ranged from 0.79 to  
 266 1.00, all  $p < 0.0500$ ;  $R = 0.83$ , 95 % CIs [0.75 0.89],  $p < 0.0001$ ). At the group level, there was  
 267 a significant main effect of stimulation intensity on  $Vdi_{max}$ . *Post-hoc* tests indicated that  
 268  $Vdi_{max}$  did not significantly differ between 90 and 100 % of stimulation intensity ( $p = 0.9997$ ).  
 269 No significant differences in  $Vdi_{max}$  was found between consecutive stimulation intensities,  
 270 except between 80 and 90 % of stimulation intensity ( $p = 0.0080$ ). Within individuals,  $Vdi_{max}$   
 271 plateaued at 90 % of stimulation intensity in 6 participants, at 80 % in one participant, and at  
 272 70 % in one participant.

273  $TFdi_{tw}$  correlated to stimulation intensity ( $R = 0.72$ , 95 % CIs [0.60 0.80],  $p < 0.0001$ ).  
 274 Individual correlations were significant in 10 out of 13 subjects ( $\rho$  ranged from 0.67 to 0.95,  
 275 all  $p < 0.05$ ;  $\rho$  ranged from 0.33 to 0.52 in the three remaining participants, all  $p > 0.2200$ ). At  
 276 the group level, there was a significant main effect of stimulation intensity on  $TFdi_{tw}$ . *Post-*  
 277 *hoc* tests showed that  $TFdi_{tw}$  did not significantly differ between 60 to 100% of stimulation  
 278 intensity (all  $p > 0.1155$ ). No significant differences in  $TFdi_{tw}$  was found between consecutive  
 279 stimulation intensities. Within individuals,  $TFdi_{tw}$  plateaued at 90 % of stimulation intensity  
 280 in 5 participants, at 80 % in two participants, at 70 % in two participants, at 50 % in one  
 281 participant and at 30 % in one participant.  $TFdi_{tw}$  and  $Vdi_{max}$  at all stimulation intensities are  
 282 shown in Figure 6B and 6C, respectively.

### 283 **Relationships between $Pdi_{tw}$ and indices derived from ultrafast ultrasound**

284 Within-individuals' relationships between  $Pdi_{tw}$  and  $Vdi_{max}$ , and between  $Pdi_{tw}$  and  
 285  $TFdi_{tw}$  are presented in Figure 7.  $Vdi_{max}$  correlated to  $Pdi_{tw}$  in all participants ( $\rho$  ranged from  
 286 0.64 to 1.00, all  $p < 0.05$ ;  $R = 0.75$ , 95 % CIs [0.65 0.83],  $p < 0.0001$ ).  $TFdi_{tw}$  positively  
 287 correlated to  $Pdi_{tw}$  ( $R = 0.69$ , 95 % CIs [0.57 0.79],  $p < 0.0001$ ) and individual correlation  
 288 coefficients were significant in 8 out of 13 participants ( $\rho$  ranged from 0.85 to 0.93, all  
 289  $p < 0.05$ ;  $\rho$  ranged from -0.27 to 0.70, in the five remaining participants, all  $p > 0.06$ ).

## 290 Discussion

291 This study is the first to image the diaphragm contraction induced by CMS using  
292 ultrafast US. The main results are as follow: i) maximal tissue velocity within the diaphragm  
293 significantly increased with stimulation intensity while diaphragm thickening fraction  
294 plateaued at low stimulation intensity, ii) intra-session reliability of maximal tissue velocity  
295 within the diaphragm was high and intra-session reliability of diaphragm thickening fraction  
296 was poor iii) twitch transdiaphragmatic pressure strongly correlated with maximal tissue  
297 velocity within the diaphragm and moderately correlated with diaphragm thickening fraction.

### 298 **Vdi<sub>max</sub> is sensitive to changes in stimulation intensity and correlates to twitch** 299 **transdiaphragmatic pressure**

300 We found that Vdi<sub>max</sub> increased with stimulation intensity in all participants. These  
301 results are in line with previous works that reported a gradual increase in tissue velocity with  
302 stimulation intensity during contractions elicited in the *biceps brachii* ([Deffieux et al., 2008](#);  
303 [Gronlund et al., 2013](#)). To the best of our knowledge, this study is the first to report the  
304 relationship between a muscle's tissue velocity and the force/pressure it produces. We found  
305 that Vdi<sub>max</sub> correlated to Pdi<sub>tw</sub> in all participants, supporting that the magnitude of Vdi<sub>max</sub> is  
306 associated with the diaphragm contractility. Interestingly, Pdi<sub>tw</sub> was supramaximal in two  
307 subjects only, whereas Vdi<sub>max</sub> was supramaximal in 8 subjects. The inability to reach  
308 supramaximal Pdi<sub>tw</sub> values in some subjects has been addressed before ([Man et al., 2004](#);  
309 [Spiesshoefer et al., 2019](#)). This may be partly explained by insufficient magnetic stimulation  
310 power to fully activate the phrenic nerves. It cannot be ruled out that supramaximality of  
311 Pdi<sub>tw</sub> occurred between 90 and 100 % of stimulation intensity. Nonetheless, it is known that  
312 CMS at highest stimulation intensities stimulates neck muscles ([Attali et al., 1997](#)). Thus,  
313 Pdi<sub>tw</sub> is likely to increase not because of a higher activation of the diaphragm, but because  
314 the recruitment of neck muscles increases the deflation of twitch Pes ([Wragg et al., 1994](#);  
315 [Laghi et al., 1996](#)). Regarding Vdi<sub>max</sub>, supramaximality was reached in 8 out of 13  
316 participants. The fact that Vdi<sub>max</sub> plateaued while Pdi<sub>tw</sub> continued to increase may be related  
317 to specificity of Vdi<sub>max</sub> measurement, which directly probe the diaphragm. Therefore, Vdi<sub>max</sub>  
318 may be considered as a specific index of diaphragm contractility following CMS, ruling out

## Ultrafast ultrasound imaging of the diaphragm

319 the confounding effects related to the recruitment of extra diaphragmatic muscle.  $V_{di_{max}}$  did  
320 not meet supramaximality criteria in 5 subjects. Interestingly, 4 out of these 5 subjects did  
321 not reach supramaximality for  $P_{di_{tw}}$  either. It can thus be suggested that the absence of  $V_{di_{max}}$   
322 supramaximality is directly related to the absence of  $P_{di_{tw}}$  supramaximality. Also, one may  
323 observe that  $V_{di}$  increases in the milliseconds following stimulation, while  $P_{di}$  peaks  $\sim 150$   
324 ms after stimulation (Figure 4). This supports that the rapid change in  $V_{di}$  correspond to  
325 diaphragm contraction and that this lag reflects the time needed for the diaphragm to transfer  
326 its force generation into an actual pressure generation. Importantly,  $V_{di_{max}}$  was found to be  
327 strongly reproducible, as indicated by low SEM and high ICC that were comparable to those  
328 observed for  $P_{di_{tw}}$  (Table 1). This high reliability build confidence regarding the potential of  
329  $V_{di_{max}}$  for non-volitional monitoring of diaphragm contractility over time. This study is also  
330 the first to report  $TF_{di_{tw}}$  values during CMS. Repeated measure correlations showed a  
331 significant correlation between  $TF_{di_{tw}}$  and stimulation intensity. Within individuals, 10 (77  
332 %) participants presented with a significant relationship between  $TF_{di_{tw}}$  and stimulation  
333 intensity. As compared to  $V_{di_{max}}$ ,  $TF_{di_{tw}}$  was shown to be less sensitive to changes in  
334 stimulation intensity. At the group level,  $TF_{di_{tw}}$  was moderately correlated to  $P_{di_{tw}}$ . Our  
335 results are in line with previous studies that reported significant relationship between  
336 diaphragm thickening fraction and changes in  $P_{di}$  during spontaneous breathing, inspiratory  
337 efforts, or in mechanically ventilated patients ([Ueki et al., 1995](#); [Vivier et al., 2012](#); [Goligher](#)  
338 [et al., 2015](#); [Umbrello et al., 2015](#)). However, when looking at individual relationship, the  
339 correlation between  $TF_{di_{tw}}$  and  $P_{di_{tw}}$  reached significance in 8 subjects (62%) only. We also  
340 found that  $TF_{di_{tw}}$  plateaued at low stimulation intensity (60%). Importantly, the intra-session  
341 reliability of  $TF_{di_{tw}}$  was rather poor. There are several potential explanations for these  
342 findings. First,  $TF_{di_{tw}}$  was computed manually by drawing the position of the *pleura* and  
343 *peritoneum*. Imprecisions during this manual step might also be amplified by the lower image  
344 quality found using ultrafast US as compared to that of conventional US imaging. More  
345 specifically, conventional US imaging uses focused pulses, allowing for high image quality  
346 but a relatively low sampling rate (a few tens per second). On the other hand, ultrafast US  
347 plane wave imaging allows very high sampling rate (here, 1 kHz) but image quality is lower  
348 ([Montaldo et al., 2009](#)). Indeed, ultrafast US prevents the focusing of US beams to a specific



349 tissue (i.e. in this case, the diaphragm) and negatively impacts the signal to noise ratio of the  
350 resulting image. As a result, the ultrafast US sequence developed for the current experiment  
351 does not allow strong contrast of anatomic structures in comparison to standard US imaging  
352 (Figure 1A). This may disrupt the measurement of  $TFdi_{tw}$  (Figure 1B) and contribute to  
353 explain the low intra-session reliability of  $TFdi_{tw}$  indicated by the substantial SEM (~10%)  
354 and moderate ICC (<0.6). Noteworthy,  $TFdi$  during ventilation was previously shown to be  
355 moderately reliable using traditional ultrasound imaging ([Goligher et al., 2015](#)). This low  
356 reliability may explain, at least in part, the absence of increase in  $TFdi_{tw}$  with increasing  
357 stimulation intensity and increasing  $Pdi_{tw}$  in some participants. Indeed, we found in some  
358 participants that  $TFdi_{tw}$  plateaued at intensities as low as 40—60 %. Because of the large  
359 increase in  $Pdi_{tw}$  between 60 and 100 % of stimulation intensity, it is very unlikely that  
360 supramaximal  $TFdi_{tw}$  values depicts full diaphragm recruitment. All together, these findings  
361 suggest that  $TFdi_{tw}$  may be of limited help to assess diaphragm contractility in response to  
362 CMS.

### 363 **Perspectives and limitations**

364 We demonstrated that  $Vdi_{max}$  was strongly related to  $Pdi_{tw}$  in all subjects. This could  
365 have important implications for monitoring temporal changes in diaphragm contractility in  
366 patients presenting with diaphragm dysfunction. In other words,  $Vdi_{max}$  elicited by CMS  
367 could be monitored over time using ultrafast US, allowing iterative, specific, fully non-  
368 invasive and non-volitional assessment of diaphragm contractility. It is worth noting that  
369 between-subject variability was relatively important. In turn, one may question how  $Vdi_{max}$   
370 may be used to identify diaphragm dysfunction. Further studies will focus on this specific  
371 point, with the perspective that  $Vdi_{max}$  may be one parameter, among others, guiding  
372 clinicians through the assessment of diaphragm contractility. Inter-operator and between day  
373 reliability of  $Vdi_{max}$  remains to be investigated. Assessing the delay between CMS and  
374 diaphragm response as assessed using  $Vdi_{max}$  may also be promising to investigate both  
375 phrenic conduction and electromechanical delay. Unfortunately, EMG was not available in  
376 the current study and this shall be investigated in future works. As mentioned above, we  
377 cannot ensure that supramaximality was achieved in all subjects. It is possible that

378 maximality occurred between 90 and 100 % of stimulation intensity in some subjects. This  
379 problem has been addressed before ([Man et al., 2004](#); [Spiesshoefer et al., 2019](#)), but can be  
380 considered negligible if a rigorous and standardized study-design is routinely used. Also, as  
381 the primary aim of this study was to detect changes in diaphragm contractility according to  
382 stimulation intensity and relationships between variables, supramaximality should not be  
383 considered as an important concern. We also emphasize that only the right hemidiaphragm  
384 was imaged in this study and that future works shall thoroughly investigate this approach in  
385 the left hemidiaphragm. Lastly, the ultrafast US sequence used in this study was custom-  
386 made so that the present approach cannot be readily generalized to clinical environments as  
387 it required a specific US scanner, US sequences that are not available commercially, specific  
388 training, and represent a non-negligible costs.

### 389 **Conclusion**

390         These study shows that ultrafast US may be used to image diaphragm behavior  
391 following CMS. Diaphragm tissue velocity is strongly correlated with twitch  
392 transdiaphragmatic pressure and appears to be highly specific to diaphragm contractility.  
393 Further research is warranted to investigate how ultrafast US may be used in patients, in  
394 particular those with diaphragm dysfunction. Coupling ultrafast US with CMS opens  
395 prospect for a fully non-invasive, non-volitional assessment and follow-up of diaphragm  
396 contractility in clinical populations.

397 **Additional information**

398 **Data Availability Statement**

399           The data that support the findings of this study are available from the corresponding  
400 author upon reasonable request.

401 **Competing interests**

402           JLG is a scientific consultant for Supersonic Imagine, Aix-en-Provence, France. MD  
403 received personal fees from Lungpacer.

404 **Fundings**

405           The PhD fellowship of TP is funded by the *Fondation EDF* that is supporting the  
406 RespiMyo project, which includes the current study. This study was also supported by the  
407 *Association Française Contre Les Myopathies* (AFM).

408 **Author contributions**

409           All authors participated in the conception and design of the study. TP and DB  
410 performed experiments. TP, JLG and DB analyzed the data and drafted the original version  
411 of the manuscript. All authors critically revised and approved the final version of the  
412 manuscript. All persons designated as authors qualify for authorship, and all those who  
413 qualify for authorship are listed.

414 **Supporting information**

415           S1. A movie clip, slowed down 40 times, showing pressure signals, M-mode images,  
416 and indices derived from ultrafast US is available at the following link:  
417 <https://figshare.com/s/fe55c9aa033cb6a42617>.

418           S2. A movie clip, in real-time, showing B-Mode and M-Mode images during a typical  
419 500-ms ultrafast ultrasound acquisition is available at the following link:  
420 <https://figshare.com/s/79fb82dd0361075df33e>

421 **References**

422

423 Agostoni E & Rahn H. (1960). Abdominal and thoracic pressures at different lung volumes.  
424 *J Appl Physiol* **15**, 1087-1092.

425

426 American Thoracic Society/European Respiratory S. (2002). ATS/ERS Statement on  
427 respiratory muscle testing. *Am J Respir Crit Care Med* **166**, 518-624.

428

429 Attali V, Mehiri S, Straus C, Salachas F, Arnulf I, Meininger V, Derenne JP & Similowski  
430 T. (1997). Influence of neck muscles on mouth pressure response to cervical magnetic  
431 stimulation. *Am J Respir Crit Care Med* **156**, 509-514.

432

433 Bachasson D, Dres M, Nierat M, Doorduyn J, Gennisson J, Hogrel J & Similowski T. (2018).  
434 Ultrafast Ultrasound Imaging Grants Alternate Methods for Assessing Diaphragm  
435 Function. In *2018 IEEE International Ultrasonics Symposium (IUS)*, pp. 1-4.

436

437 Bachasson D, Dres M, Nierat MC, Gennisson JL, Hogrel JY, Doorduyn J & Similowski T.  
438 (2019). Diaphragm shear modulus reflects transdiaphragmatic pressure during  
439 isovolumetric inspiratory efforts and ventilation against inspiratory loading. *J Appl*  
440 *Physiol (1985)* **126**, 699-707.

441

442 Bakdash JZ & Marusich LR. (2017). Repeated Measures Correlation. *Front Psychol* **8**, 456.

443

444 Baydur A, Behrakis PK, Zin WA, Jaeger M & Milic-Emili J. (1982). A simple method for  
445 assessing the validity of the esophageal balloon technique. *Am Rev Respir Dis* **126**,  
446 788-791.

## Ultrafast ultrasound imaging of the diaphragm

447

448 Deffieux T, Gennisson JL, Tanter M & Fink M. (2008). Assessment of the mechanical  
449 properties of the musculoskeletal system using 2-D and 3-D very high frame rate  
450 ultrasound. *IEEE Trans Ultrason Ferroelectr Freq Control* **55**, 2177-2190.

451

452 Dres M & Demoule A. (2020). Monitoring diaphragm function in the ICU. *Curr Opin Crit  
453 Care* **26**, 18-25.

454

455 Geary CM, Welch JF, McDonald MR, Peters CM, Leahy MG, Reinhard PA & Sheel AW.  
456 (2019). Diaphragm fatigue and inspiratory muscle metaboreflex in men and women  
457 matched for absolute diaphragmatic work during pressure-threshold loading. *J  
458 Physiol* **597**, 4797-4808.

459

460 Goligher EC, Laghi F, Detsky ME, Farias P, Murray A, Brace D, Brochard LJ, Bolz SS,  
461 Rubenfeld GD, Kavanagh BP & Ferguson ND. (2015). Measuring diaphragm  
462 thickness with ultrasound in mechanically ventilated patients: feasibility,  
463 reproducibility and validity. *Intensive Care Med* **41**, 642-649.

464

465 Gronlund C, Claesson K & Holtermann A. (2013). Imaging two-dimensional mechanical  
466 waves of skeletal muscle contraction. *Ultrasound Med Biol* **39**, 360-369.

467

468 Hamnegaard CH, Wragg S, Kyroussis D, Mills G, Bake B, Green M & Moxham J. (1995).  
469 Mouth pressure in response to magnetic stimulation of the phrenic nerves. *Thorax* **50**,  
470 620-624.

471

472 Hopkins W. (2002). A new view of statistics: Effect magnitudes. Retrieved February 14,  
473 2005.

474

475 Kabitz HJ, Walker D, Walterspacher S & Windisch W. (2007). Controlled twitch mouth  
476 pressure reliably predicts twitch esophageal pressure. *Respir Physiol Neurobiol* **156**,  
477 276-282.

478

479 Laghi F, Harrison MJ & Tobin MJ. (1996). Comparison of magnetic and electrical phrenic  
480 nerve stimulation in assessment of diaphragmatic contractility. *J Appl Physiol (1985)*  
481 **80**, 1731-1742.

482

483 Laveneziana P, Albuquerque A, Aliverti A, Babb T, Barreiro E, Dres M, Dubé B-P, Fauroux  
484 B, Gea J, Guenette JA, Hudson AL, Kabitz H-J, Laghi F, Langer D, Luo Y-M, Alberto  
485 Neder J, O'Donnell D, Polkey MI, Rabinovich RA, Rossi A, Series F, Similowski T,  
486 Spengler C, Vogiatzis I & Verges S. (2019). ERS Statement on Respiratory Muscle  
487 Testing at Rest and during Exercise. *European Respiratory Journal*, 1801214.

488

489 Loupas T, Powers JT & Gill RW. (1995). An axial velocity estimator for ultrasound blood  
490 flow imaging, based on a full evaluation of the Doppler equation by means of a two-  
491 dimensional autocorrelation approach. *IEEE Transactions on Ultrasonics,*  
492 *Ferroelectrics, and Frequency Control* **42**, 672-688.

493

494 Man WD, Moxham J & Polkey MI. (2004). Magnetic stimulation for the measurement of  
495 respiratory and skeletal muscle function. *Eur Respir J* **24**, 846-860.

496

497 Mojoli F, Chiumello D, Pozzi M, Algieri I, Bianzina S, Luoni S, Volta CA, Braschi A &  
498 Brochard L. (2015). Esophageal pressure measurements under different conditions of  
499 intrathoracic pressure. An in vitro study of second generation balloon catheters.  
500 *Minerva Anesthesiol* **81**, 855-864.

501

## Ultrafast ultrasound imaging of the diaphragm

502 Montaldo G, Tanter M, Bercoff J, Benech N & Fink M. (2009). Coherent plane-wave  
503 compounding for very high frame rate ultrasonography and transient elastography.  
504 *IEEE Trans Ultrason Ferroelectr Freq Control* **56**, 489-506.

505

506 Oppersma E, Hatam N, Doorduyn J, van der Hoeven JG, Marx G, Goetzenich A, Fritsch S,  
507 Heunks LMA & Bruells CS. (2017). Functional assessment of the diaphragm by  
508 speckle tracking ultrasound during inspiratory loading. *J Appl Physiol (1985)* **123**,  
509 1063-1070.

510

511 R Core Team. (2020). R: A Language and Environment for Statistical Computing. R  
512 Foundation for Statistical Computing, Vienna, Austria.

513

514 Rossi S, Hallett M, Rossini PM & Pascual-Leone A. (2011). Screening questionnaire before  
515 TMS: an update. *Clin Neurophysiol* **122**, 1686.

516

517 Sandrin L, Catheline S, Tanter M, Hennequin X & Fink M. (1999). Time-resolved pulsed  
518 elastography with ultrafast ultrasonic imaging. *Ultrason Imaging* **21**, 259-272.

519

520 Shahgholi L, Baria MR, Sorenson EJ, Harper CJ, Watson JC, Strommen JA & Boon AJ.  
521 (2014). Diaphragm depth in normal subjects. *Muscle Nerve* **49**, 666-668.

522

523 Similowski T, Fleury B, Launois S, Cathala HP, Bouche P & Derenne JP. (1989). Cervical  
524 magnetic stimulation: a new painless method for bilateral phrenic nerve stimulation  
525 in conscious humans. *J Appl Physiol (1985)* **67**, 1311-1318.

526

## Ultrafast ultrasound imaging of the diaphragm

- 527 Similowski T, Gauthier AP, Yan S, Macklem PT & Bellemare F. (1993). Assessment of  
528 diaphragm function using mouth pressure twitches in chronic obstructive pulmonary  
529 disease patients. *Am Rev Respir Dis* **147**, 850-856.
- 530
- 531 Spiesshoefer J, Henke C, Herkenrath S, Brix T, Randerath W, Young P & Boentert M.  
532 (2019). Transdiaphragmatic pressure and contractile properties of the diaphragm  
533 following magnetic stimulation. *Respir Physiol Neurobiol* **266**, 47-53.
- 534
- 535 Teixeira A, Demoule A, Verin E, Morelot-Panzini C, Series F, Straus C & Similowski T.  
536 (2007). Superiority of nasal mask pressure over mouth pressure, as a surrogate of  
537 diaphragm twitch-related esophageal pressure, in healthy humans. *Respir Physiol*  
538 *Neurobiol* **159**, 236-240.
- 539
- 540 Tuinman PR, Jonkman AH, Dres M, Shi ZH, Goligher EC, Goffi A, de Korte C, Demoule A  
541 & Heunks L. (2020). Respiratory muscle ultrasonography: methodology, basic and  
542 advanced principles and clinical applications in ICU and ED patients-a narrative  
543 review. *Intensive Care Med* **46**, 594-605.
- 544
- 545 Ueki J, De Bruin PF & Pride NB. (1995). In vivo assessment of diaphragm contraction by  
546 ultrasound in normal subjects. *Thorax* **50**, 1157-1161.
- 547
- 548 Umbrello M, Formenti P, Longhi D, Galimberti A, Piva I, Pezzi A, Mistraretti G, Marini JJ  
549 & Iapichino G. (2015). Diaphragm ultrasound as indicator of respiratory effort in  
550 critically ill patients undergoing assisted mechanical ventilation: a pilot clinical study.  
551 *Crit Care* **19**, 161.
- 552



## Ultrafast ultrasound imaging of the diaphragm

553 Vivier E, Mekontso Dessap A, Dimassi S, Vargas F, Lyazidi A, Thille AW & Brochard L.  
554 (2012). Diaphragm ultrasonography to estimate the work of breathing during non-  
555 invasive ventilation. *Intensive Care Med* **38**, 796-803.

556

557 Welch JF, Archiza B, Guenette JA, West CR & Sheel AW. (2018). Sex differences in  
558 diaphragmatic fatigue: the cardiovascular response to inspiratory resistance. *J Physiol*  
559 **596**, 4017-4032.

560

561 Windisch W, Kabitz HJ & Sorichter S. (2005). Influence of different trigger techniques on  
562 twitch mouth pressure during bilateral anterior magnetic phrenic nerve stimulation.  
563 *Chest* **128**, 190-195.

564

565 Wragg S, Aquilina R, Moran J, Ridding M, Hamnegard C, Fearn T, Green M & Moxham J.  
566 (1994). Comparison of cervical magnetic stimulation and bilateral percutaneous  
567 electrical stimulation of the phrenic nerves in normal subjects. *Eur Respir J* **7**, 1788-  
568 1792.

569

570 Yan S, Gauthier AP, Similowski T, Macklem PT & Bellemare F. (1992). Evaluation of  
571 human diaphragm contractility using mouth pressure twitches. *Am Rev Respir Dis*  
572 **145**, 1064-1069.

573

574

575 **Tables**

576 **Table 1.** Within day reliability of twitch transdiaphragmatic pressure ( $P_{di_{tw}}$ ), maximal  
 577 diaphragm tissue velocity ( $V_{di_{max}}$ ) and diaphragm thickening fraction ( $TF_{di_{tw}}$ ) for all  
 578 stimulations. SEM, standard error of measurement; ICC, intraclass correlation coefficient;  
 579 [95% CI], 95% confidence interval.

580

Variable	Mean (SD)	SEM [95 % CI]	ICC [95 % CI]
$P_{di_{tw}}$ (cmH <sub>2</sub> O)	11.6 (9.5)	1.55 [1.39 ; 1.75]	0.97 [0.96 ; 0.98]
$V_{di_{max}}$ (mm.s <sup>-1</sup> )	5.6 (5.0)	1.89 [1.70 ; 2.13]	0.86 [0.81 ; 0.90]
$TF_{di_{tw}}$ (%)	18.7 (15.6)	10.41 [9.38 ; 11.76]	0.56 [0.43 ; 0.66]

581

582

583 **Figures**

584 **Figure 1.** A. Typical B-Mode image of the diaphragm using conventional ultrasound  
 585 imaging. Conventional ultrasound uses focused pulses, allowing high image quality but  
 586 relatively low sampling rate (a few tens per second). The diaphragm can be identified as a  
 587 three-layers structure superficial to the liver. The echogenic *pleura* and *peritoneum* layers  
 588 surround the muscular layer of the diaphragm. B. The diaphragm is imaged using the custom  
 589 ultrafast ultrasound sequence used in this study. Noteworthy, ultrafast ultrasound allows very  
 590 high frame rate but limited contrast of anatomic structures in comparison to standard US  
 591 imaging.

592 **Figure 2.** Experimental setup and procedure for recording pressure and ultrafast ultrasound  
 593 images. The participants were asked to bend their neck forward and the central hole of the  
 594 coil was positioned on the spinous process of the seventh cervical vertebra. Recording of  
 595 pressure signals was initiated 1000 ms before the onset of ultrasound recording. Cervical  
 596 magnetic stimulation was applied 100 ms after the onset of a 500-ms ultrafast ultrasound  
 597 acquisition.

598 **Figure 3.** Diaphragm tissue velocity ( $V_{di}$ ) over time along the longitudinal axis of the  
 599 ultrasound probe. Cervical magnetic stimulation occurs at 100 ms and is indicated by the  
 600 grey ribbon.

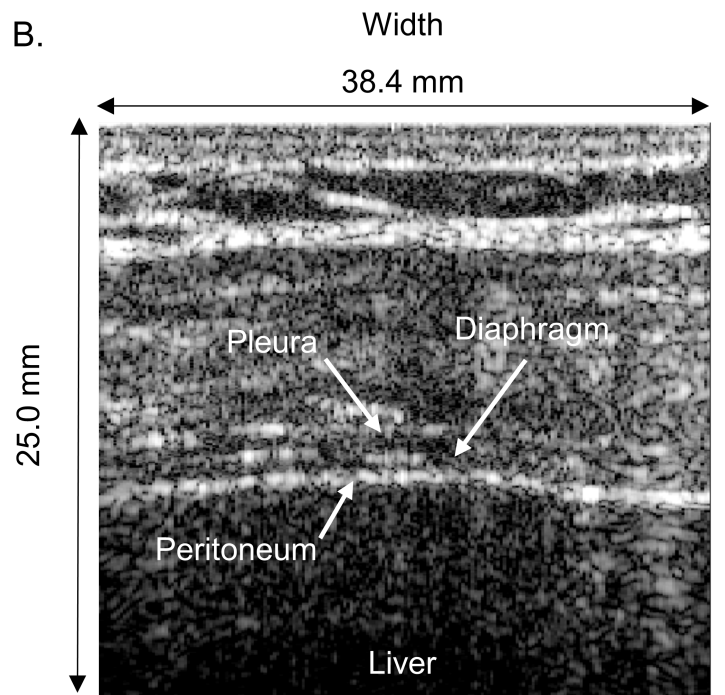
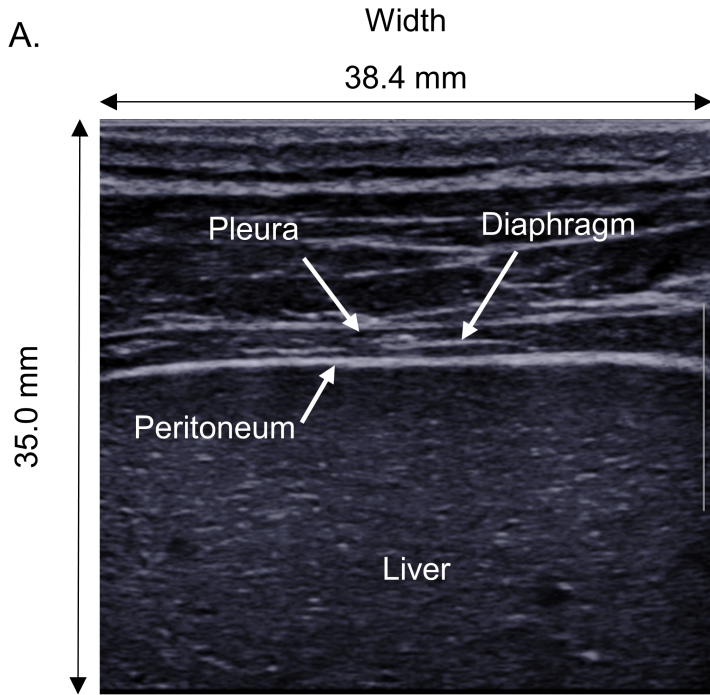
601 **Figure 4.** Typical ultrasound and physiological recordings at 40 (left), 70 (center) and 100  
 602 % (right) of stimulator intensity. The central pixel of each B-Mode image was used to  
 603 generate the M-Mode images (upper panel). *Pleura* (dashed) and *peritoneum* (solid) layers  
 604 displacement are presented in the second panel. Diaphragm tissue velocity ( $V_{di}$ ) is presented  
 605 in the third panel. Lastly, the transdiaphragmatic ( $P_{di}$ ), esophageal ( $P_{es}$ ) and gastric ( $P_{ga}$ )  
 606 pressures are displayed in the bottom panel. The dotted vertical lines at 100 ms indicate the  
 607 onset of cervical magnetic stimulation.

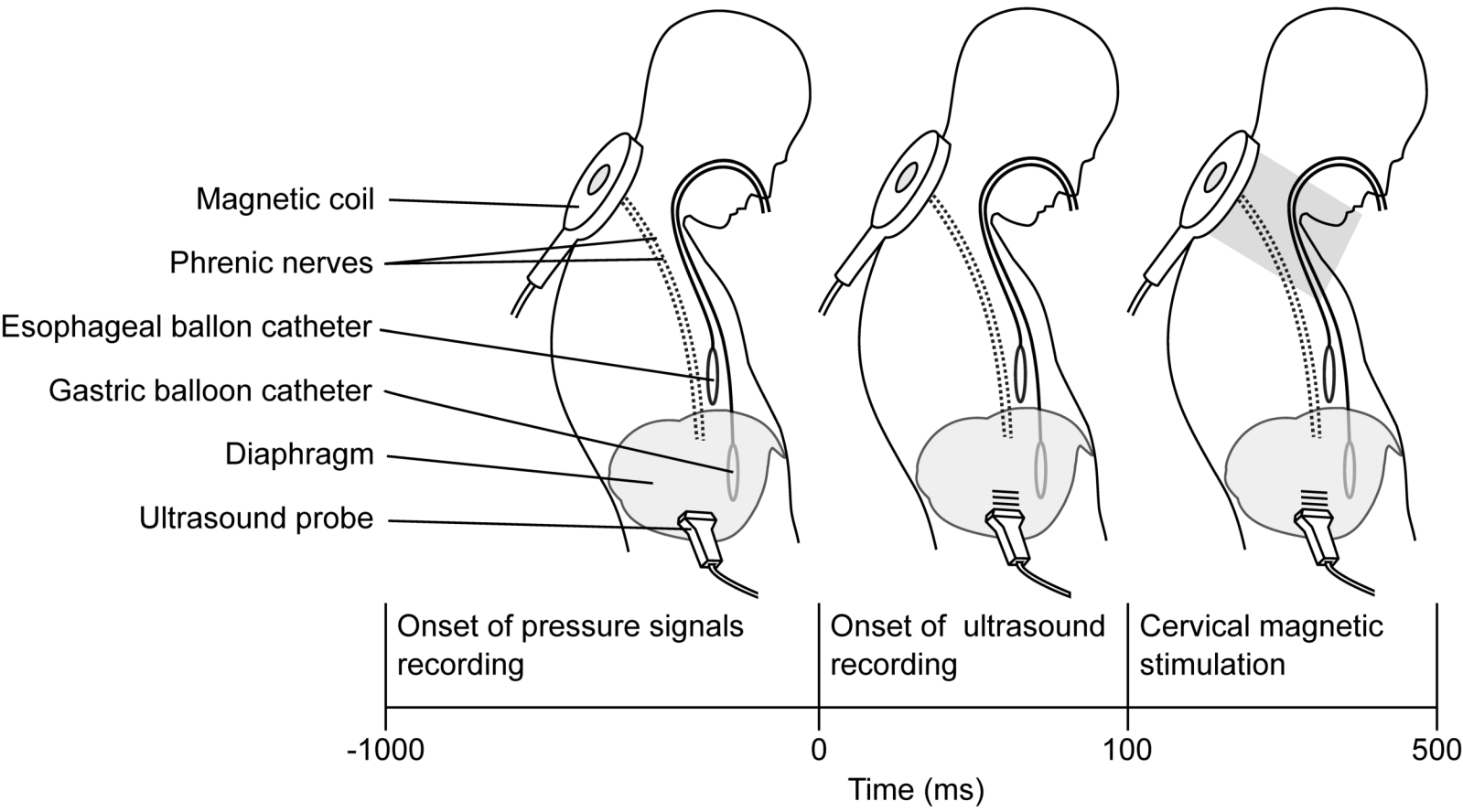
608 **Figure 5.** Esophageal ( $P_{estw}$ , A.) and gastric ( $P_{gaw}$ , B.) twitch pressures at different  
 609 stimulation intensities. Box plots present first and third quartiles, in addition to the median.  
 610 The range over which the data spread out is defined by the whiskers.

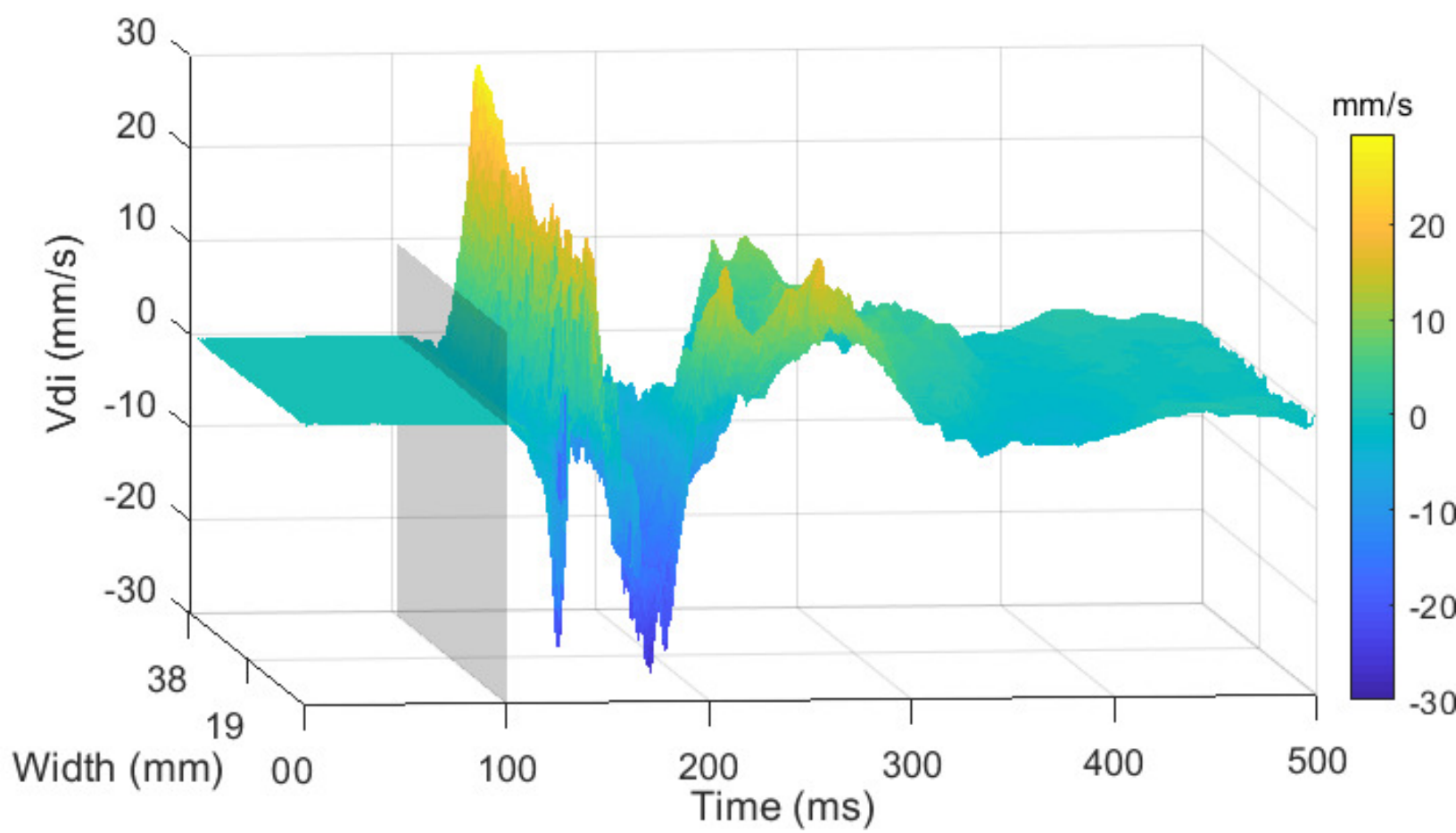
## Ultrafast ultrasound imaging of the diaphragm

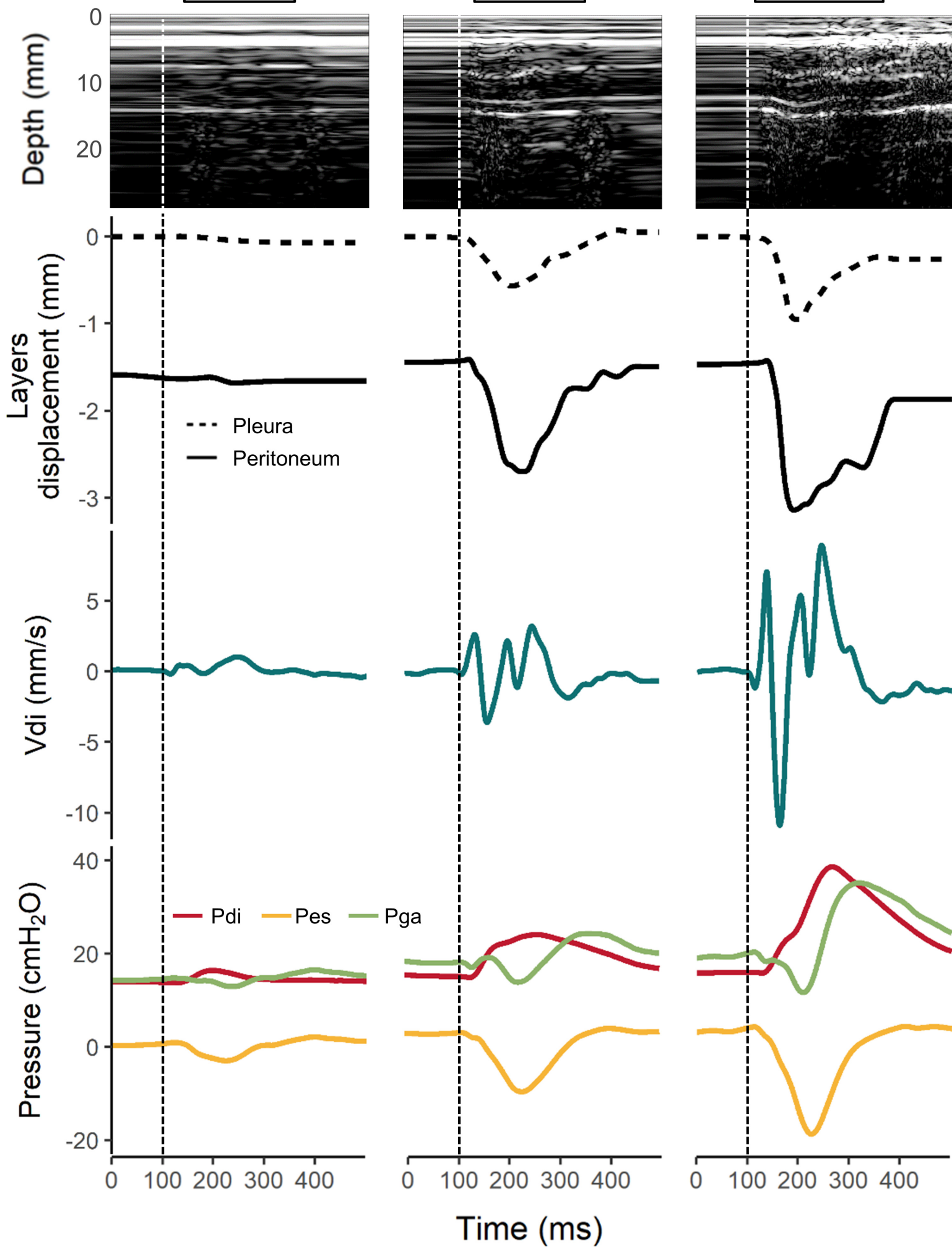
611 **Figure 6.** Twitch transdiaphragmatic pressure ( $P_{di_{tw}}$ , A.), maximal diaphragm tissue velocity  
612 ( $V_{di_{max}}$ , B.), and diaphragm thickening fraction ( $TF_{di_{tw}}$ , C.) according to stimulation  
613 intensities. Box plots present first and third quartiles, in addition to the median. The range  
614 over which the data spread out is defined by the whiskers. Repeated measure ANOVAs were  
615 used to assess the effect of stimulation intensity on  $P_{di_{tw}}$ ,  $V_{di_{max}}$ , and  $TF_{di_{tw}}$ . Tukey's *post-*  
616 *hoc* tests were conducted if a significant main effect of intensity was found. \*, significant  
617 difference with the preceding stimulation intensity (i.e. -10 %); #, significant difference with  
618 the second preceding stimulation intensity (i.e. -20 %). Averaged data points for each  
619 participant are displayed for  $P_{di_{tw}}$  (D.),  $V_{di_{max}}$  (E.), and  $TF_{di_{tw}}$  (F.). Red points on panels D,  
620 E, and F indicate supramaximality for the given parameter.

621 **Figure 7.** Averaged data points for each participant regarding the relationships between  
622 twitch transdiaphragmatic pressure ( $P_{di_{tw}}$ ) and maximal diaphragm tissue velocity ( $V_{di_{max}}$ ,  
623 A.) and between  $P_{di_{tw}}$  and diaphragm thickening fraction ( $TF_{di_{tw}}$ , B.).



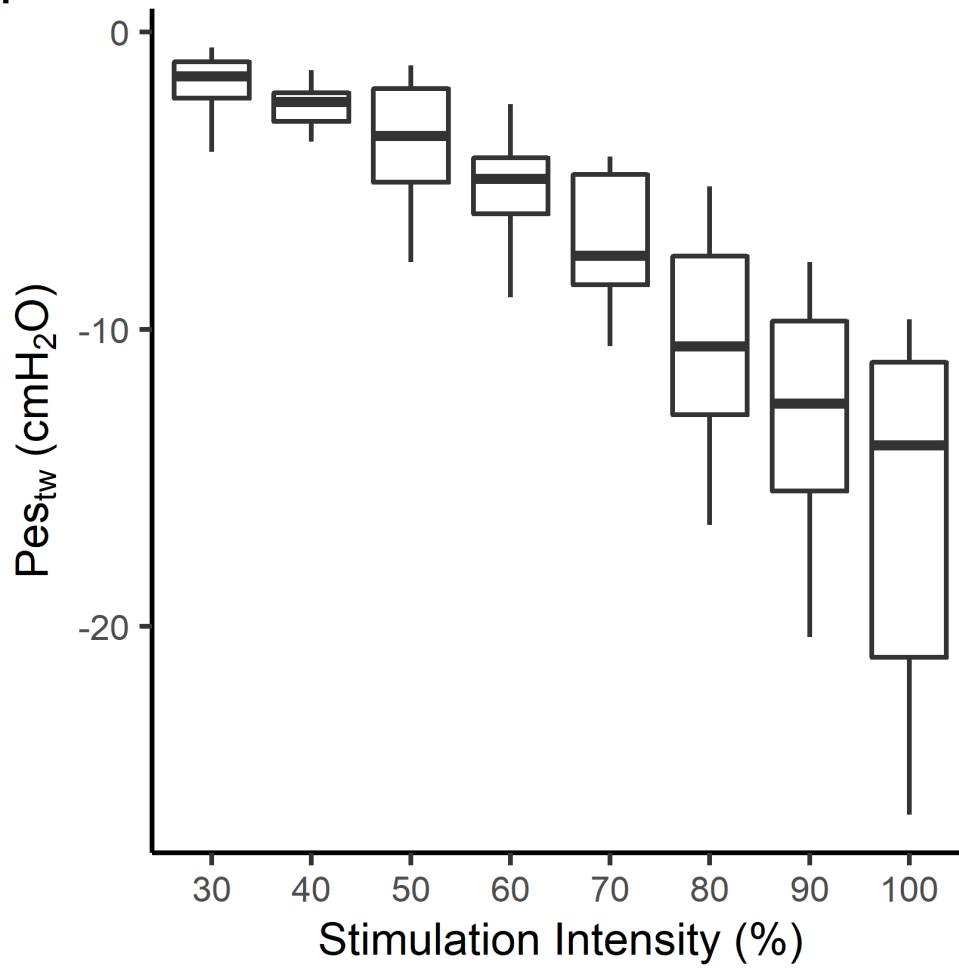




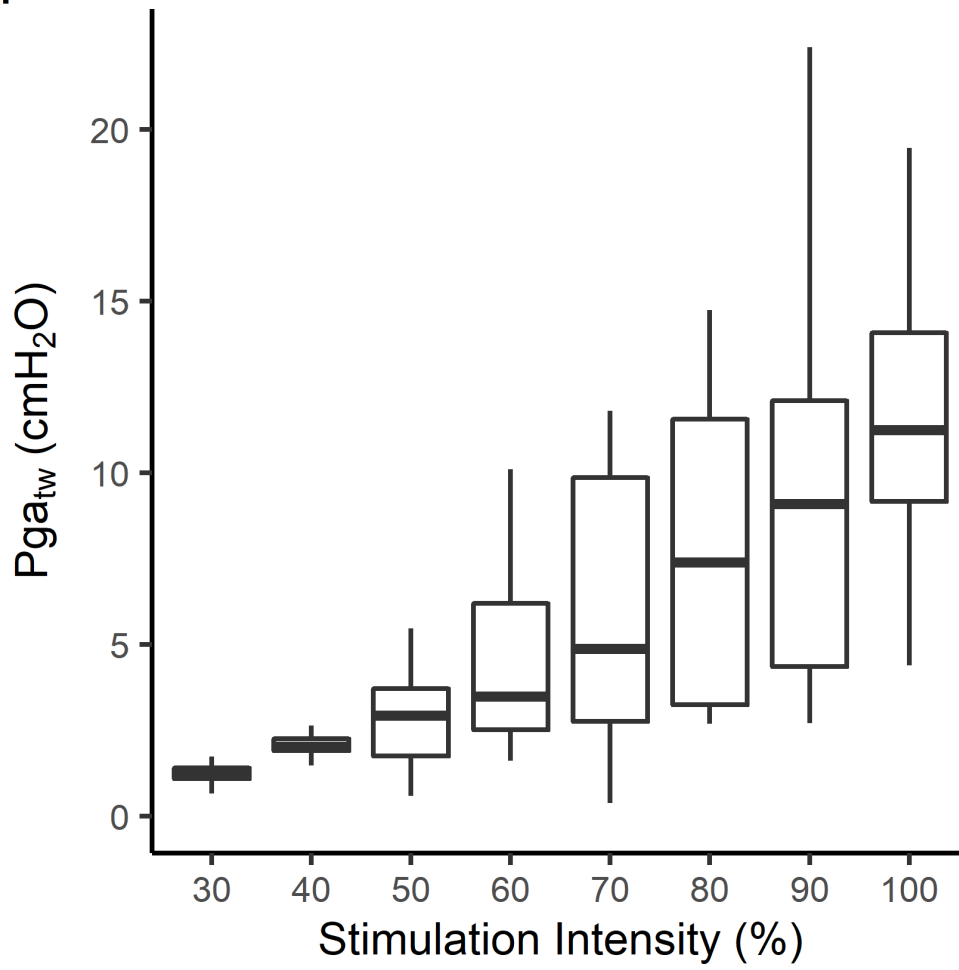
**40 %****70 %****100 %**

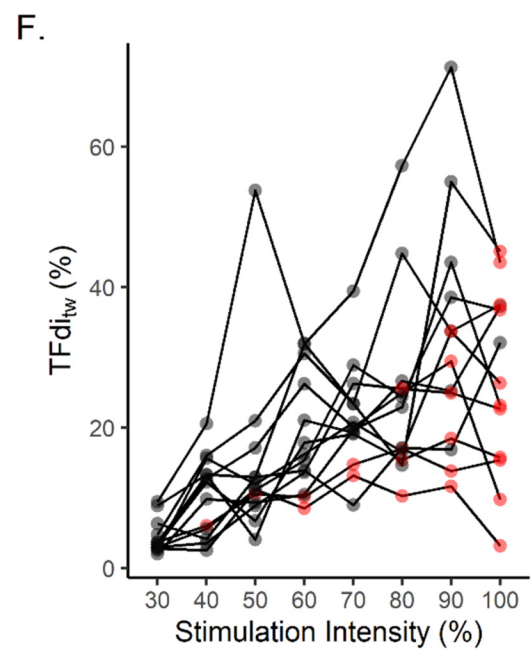
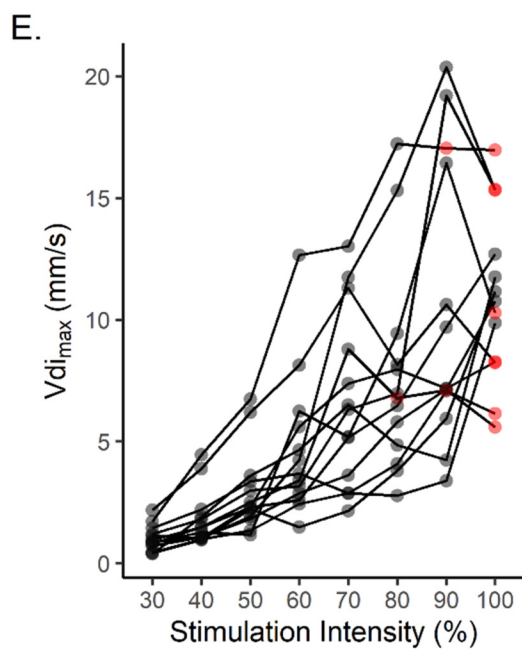
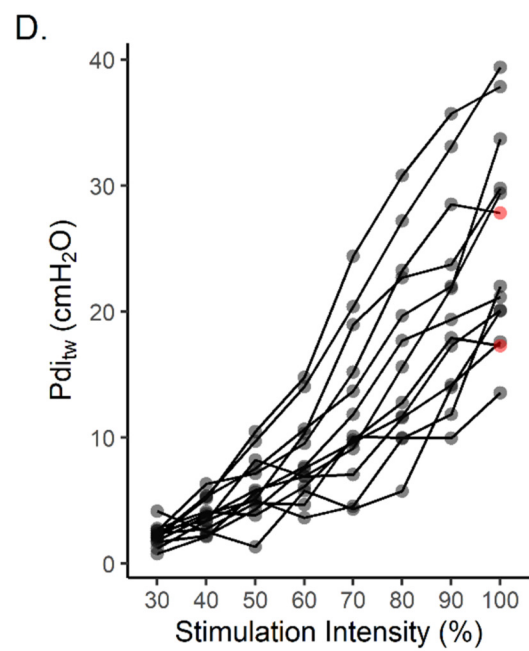
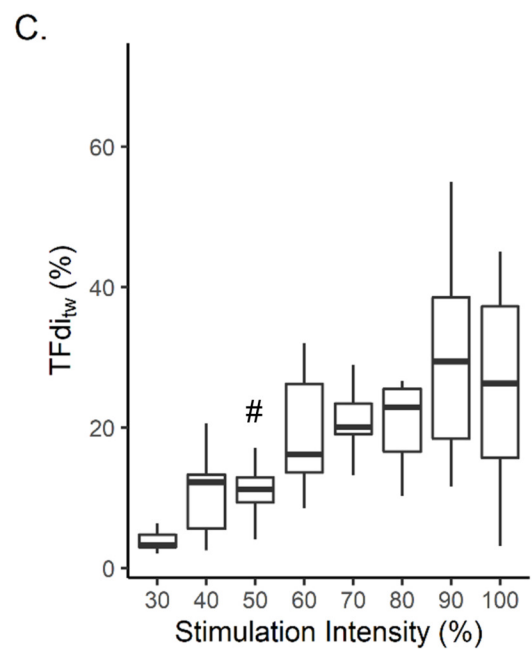
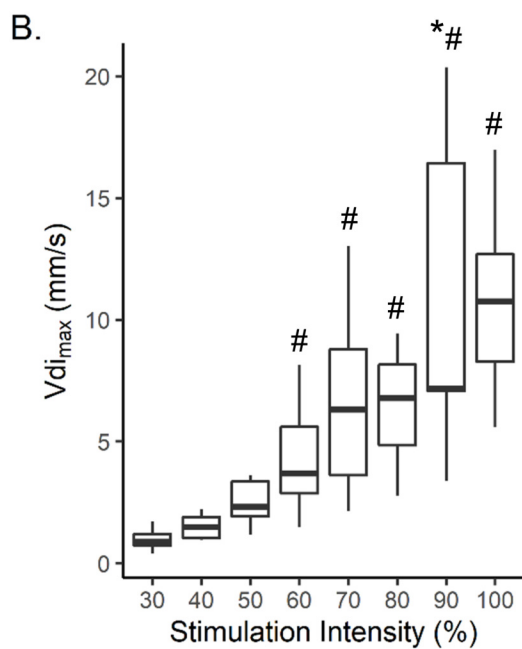
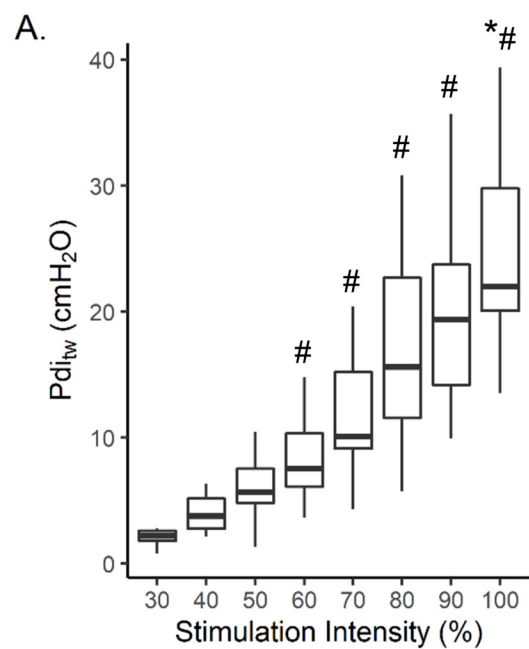


A.

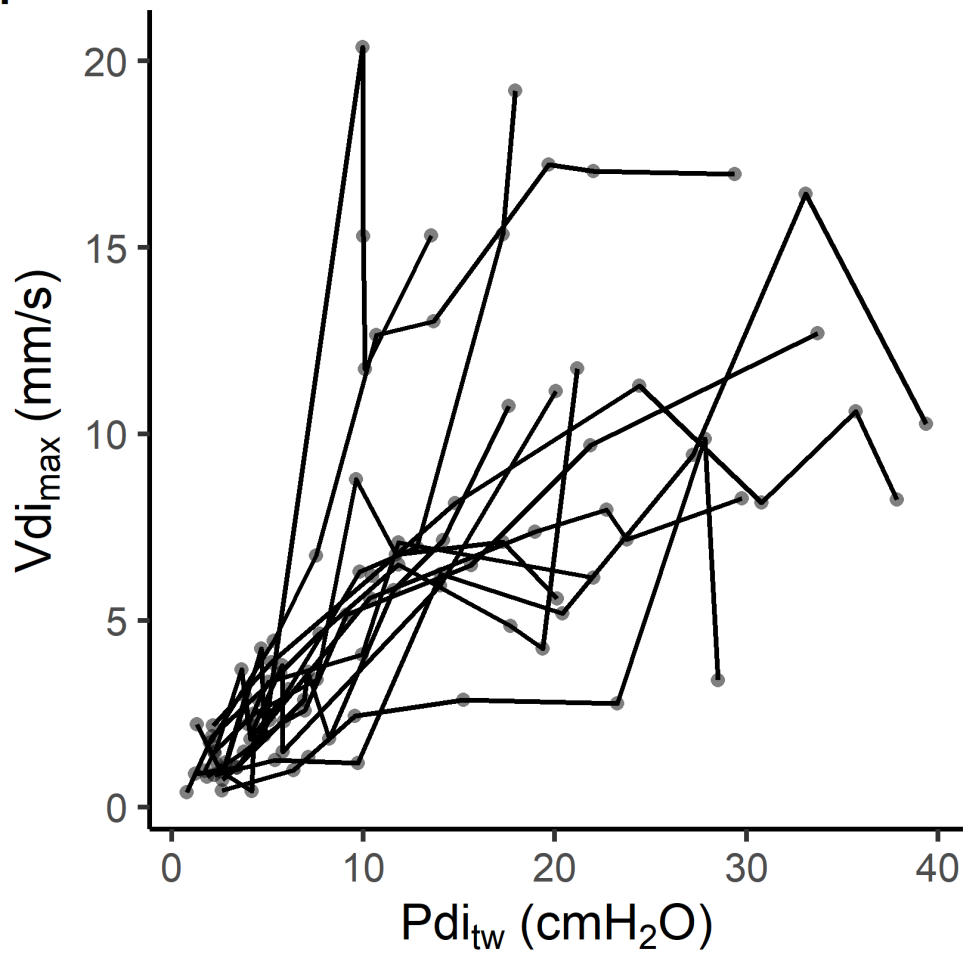


B.





A.



B.

